Defence Science Journal, Vol. 67, No. 2, March 2017, pp. 198-206, DOI : 10.14429/dsj.67.10374

Dynamic Inversion Control for Performing Herbst Manoeuver with Lateral Center-of-Gravity Offset

Bijoy K. Mukherjee[#] and Manoranjan Sinha

Department of Aerospace Engineering, IIT Kharagpur, India
[#]*E-mail: bjoy.here@gmail.com*

ABSTRACT

The present study addresses the effects of lateral center-of-gravity (CG) movement, resulting from asymmetric firing of some of the onboard stores, on the dynamics and control of a combat aircraft while attempting the highly demanding Herbst manoeuver. The complete six degree-of-freedom equations of motion of the aircraft for such lateral CG offset are derived in two different body reference frames attached either to the symmetric nominal CG location or to the shifted asymmetric CG location. The Herbst manoeuver is first simulated using nonlinear dynamic inversion based control to handle the highly nonlinear post stall flight dynamics considering the standard equation of motion without considering any lateral CG variation. Thereafter, it is observed that if the same controller is retained, the manoeuver performance deteriorates significantly even when the CG undergoes a moderate lateral shift. To overcome this shortfall, closed loop controllers are next designed incorporating both the models of asymmetric dynamics as derived in this paper. It is validated through MATLAB simulations that both the controls, thus designed, can recover the original manoeuver performance almost completely; however, the first one requires more complex computations and hence increased computation time while the second one requires that all the measurements be transformed to the new body reference frame at every time step.

Keywords: Six degree-of-freedom dynamics; Lateral center-of-gravity; Herbst manoeuver; Dynamic inversion control

NOMENCLATURE

CG	Center-of-gravity (or center-of-mass, cm)
NDI	Nonlinear dynamic inversion
o'	Nominal symmetric CG location
$\tilde{r}_0 \triangleq [x_0 \quad y_0 \quad z_0]^T$	Position of the store from o' (m)
$\tilde{r}_{cm} \triangleq [x_{cm} \quad y_{cm} \quad z_{cm}]^T$	Position of the actual CG from o' (m)
$\tilde{V}_{o'} \triangleq [u \quad v \quad w]^T$	Aircraft velocity in the body frame attached to o' (*m/s*)
$\tilde{V}_{cm} \triangleq [u' \quad v' \quad w']^T$	Aircraft velocity in the body frame attached to the CG (*m/s*)
$\tilde{\omega} \triangleq [p \quad q \quad r]^T$	Angular velocity with components in the body axes (*rad/s*)
$[I'], [I^{cm}]$	Inertia of the aircraft with the store in the frame fixed at o' or CG (*kg-m*^{2})
m, m_0	Nominal mas of the aircraft and mass of the store (*kg*)
α, β	Angle-of-attack (AOA) and sideslip angle (*rad*)
μ, γ, χ	Velocity axis bank, flight path, and heading angles (*rad*)
$\tilde{F}, \tilde{M}$	External force and moment vectors (*N, N-m*)

Received : 21 July 2016, Revised : 01 December 2016
Accepted : 15 December 2016, Online published : 11 March 2017

1. INTRODUCTION

To be effective in today's increasingly challenging combat missions, modern fighter aircraft must be able to perform various complex and rapid manoeuvers. This invariably makes them operate at high angle-of-attack (AOA) regions. In such flight regimes, aircraft flight dynamics becomes highly nonlinear because of aerodynamic and trigonometric nonlinearities in addition to inertial and kinematic couplings. Such high nonlinearities along with the reduced effectiveness of the aerodynamic controls at high AOA regions make the control design and implementation task very challenging calling for use of nonlinear control techniques in place of the conventional gain scheduled linearised controls. The situation may aggravate further when the aircraft undergoes lateral center-of-gravity (CG) movement arising from asymmetric firing of some of the onboard stores and/or asymmetric wing damage. The closed loop system should be able to effectively handle such challenges so that the aircraft can still complete its mission successfully. Design of closed loop control schemes for such asymmetric dynamics is of significant practical importance as it can potentially remove the necessity of firing the stores in pairs or carrying some dummies altogether.

Though the dynamics for laterally asymmetric CG position has been modelled from the perspective of structural damage by some researchers recently[1,2], exhaustive modelling from the first principle of the asymmetric dynamics due to asymmetric firing of stores is not available in the literature. Moreover,

some researchers[2-4] have considered only the linearised model of the asymmetric dynamics for closed loop control design purposes as some simple flight objective such as steady wings level trim was considered. Various nonlinear control methods such as the dynamic inversion or the sliding mode have been applied without considering the lateral CG variation effects by various researchers over the past two decades[5-9]. However, dynamic inversion based nonlinear control design for a combat aircraft performing some demanding post stall manoeuvers such as the Herbst with such laterally asymmetric CG location, as addressed in this paper, is a completely novel attempt.

2. AIRCRAFT DYNAMICS UNDER LATERALLY ASYMMETRIC CG

Conventional 6-DOF modelling of the aircraft dynamics is carried out assuming the CG of the aircraft to be located in the plane of symmetry[10,11]. This results in a set of simplified equations of motion as some product of inertia terms vanish. However, if the CG is located of the plane of symmetry, then the products of inertia about the body axes do not vanish leading to complicated aircraft dynamics equations. In such a situation, the body reference frame may be fixed either at the nominal CG lying in the plane of symmetry or alternately, at the shifted CG lying off the plane of symmetry. However, fixing the body frame at the actual shifted CG location is not a good idea as this point may not be fixed in the body; it may continuously vary if continuous ejection of mass or ejection of a series of stores over certain duration of time is considered. Moreover, the state variables must be redefined about this new location, while the aerodynamic quantities such as AOA, sideslip angle etc. need to be continued to be defined with respect to the nominal symmetrical CG location as the aerodynamics of the aircraft depends on the geometric configuration and not on the mass distribution. Therefore, although both of the representations are equivalent, the former one is preferable.

2.1 Body Axes Fixed at the Nominal CG

Let a general situation be considered, as shown in Fig. 1(a), where a store of mass m_0 is located at a distance $\tilde{r}_0$ from the origin o' of the body reference frame $x_b y_b z_b$. The origin of the body frame is taken to be the CG of the body if the store m_0 were absent. Due to the presence of the store, the actual CG of the aircraft lies at a distance say, $\tilde{r}_{cm}$ from o'. Other usual assumptions such as flat non-rotating Earth and rigid aircraft body are, however, retained. Let XYZ denote the Earth fixed inertial frame, m the mass of the aircraft without the store and $\tilde{\omega}$ be the angular velocity vector of the aircraft with components p, q, r resolved along the body axes. Linear velocity of an elemental mass dm at a distance $\tilde{r}$ from o' is given by

$$\tilde{V} = \tilde{V}_{o'} - S(\tilde{\omega})\tilde{r} \tag{1}$$

where $\tilde{V}_{o'}$ is the velocity of the origin of the body frame and $S(\tilde{\omega})$ is the skew-symmetric matrix notation of the vector cross product operator $(-\vec{\omega}\times)$. Therefore, linear momentum of the element is given by

$$d\tilde{P} = \tilde{V}_{o'}dm - S(\tilde{\omega})\tilde{r}\,dm \tag{2}$$

Integrating Eqn. (2) over the whole body with mass m

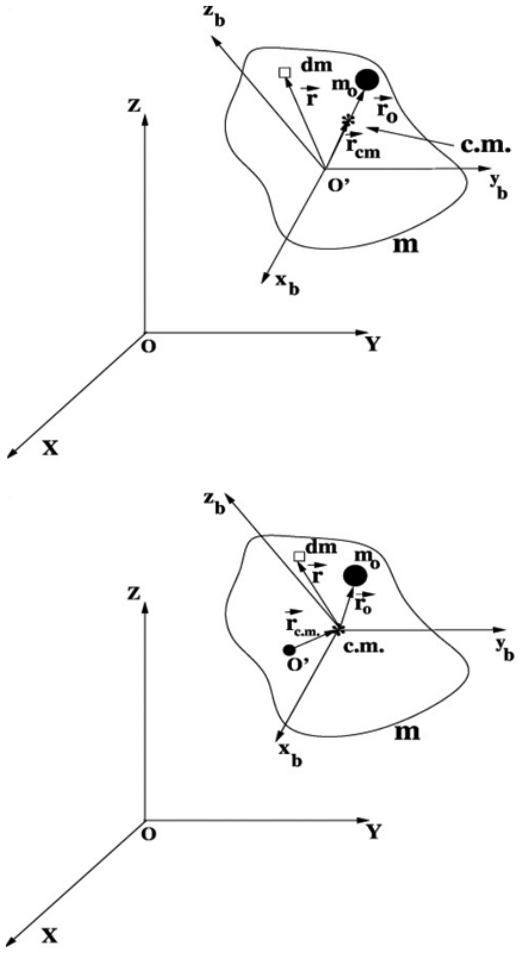

Figure 1. Schematic of rigid bodies in an inertial frame (XYZ); body frame ($x_b y_b z_b$) is fixed in the body at (a) o' and (b) the CG.

and the store m_0 (which is assumed to be a point mass) and assuming $m+m_0 = m'$, we get the total linear momentum of the whole body to be

$$\tilde{P} = m'\tilde{V}_{o'} - m_0 S(\tilde{\omega})\tilde{r}_0 \tag{3}$$

$$= m'\tilde{V}_{o'} - m'S(\tilde{\omega})\tilde{r}_{cm} \tag{4}$$

Eqn. (4) can be differentiated in the inertial frame to obtain the force equation as

$$\tilde{F} = \left.\frac{d}{dt}\right|_I m'\left(\tilde{V}_{o'} - S(\tilde{\omega})\tilde{r}_{cm}\right) \tag{5}$$

$$= m'\left(\left.\frac{d}{dt}\right|_B \left(\tilde{V}_{o'} - S(\tilde{\omega})\tilde{r}_{cm}\right) - S(\tilde{\omega})\tilde{V}_{o'} + S(\tilde{\omega})S(\tilde{\omega})\tilde{r}_{cm}\right) \tag{6}$$

$$= m'\left(\dot{\tilde{V}}_{o'_B} - S(\dot{\tilde{\omega}})\tilde{r}_{cm} - S(\tilde{\omega})\tilde{V}_{o'} + S(\tilde{\omega})S(\tilde{\omega})\tilde{r}_{cm}\right) \tag{7}$$

$$\dot{\tilde{V}}_{o'_B} + S(\tilde{r}_{cm})\dot{\tilde{\omega}} = S(\tilde{\omega})\tilde{V}_{o'} - S(\tilde{\omega})S(\tilde{\omega})\tilde{r}_{cm} + \frac{1}{m'}\tilde{F} \tag{8}$$

where $\dot{\tilde{V}}_{o'_B}$ is the linear acceleration resolved along the body frame.

Now, angular momentum of the mass element dm about the origin of the inertial frame o is given by

$$d\tilde{h}_i = -S(\tilde{r} + \tilde{r}_c)d\tilde{P} \tag{9}$$

$$= -S(\tilde{r})\tilde{V}_{o'}dm + S(\tilde{r})S(\tilde{\omega})\tilde{r}\,dm - S(\tilde{r}_c)d\tilde{P} \tag{10}$$

where $\tilde{r}_c$ denotes the position vector of the origin of the body frame o' with respect to the inertial frame. Hence, the angular momentum of the entire body is given by

$$\tilde{h}_i = -\int_B S(\tilde{r})\tilde{V}_{o'}dm + \int_B S(\tilde{r})S(\tilde{\omega})\tilde{r}\,dm - S(\tilde{r}_c)\tilde{P} \tag{11}$$

where $\int_B$ stands for integration over the whole body. The first integral on the right hand side of Eqn. (11) can be expressed as

$$\tilde{h}_1 = -\int_B S(\tilde{r})\tilde{V}_{o'}dm \tag{12}$$

$$= -\int_{NB} S(\tilde{r})\tilde{V}_{o'}dm - m_0 S(\tilde{r}_0)\tilde{V}_{o'} \tag{13}$$

$$= -m'S(\tilde{r}_{cm})\tilde{V}_{o'} \tag{14}$$

where $\int_{NB}$ denotes integral over the nominal body i.e. the body without the attached mass m_0. The second integral in Eqn. (11) can be simplified as

$$\tilde{h}_2 = -\int_B S(\tilde{r})S(\tilde{r})\tilde{\omega}dm \tag{15}$$

$$= [I']\tilde{\omega} \tag{16}$$

where $[I']$ is the inertia matrix of the entire body about the body axes. Substituting $\tilde{h}_1$ and $\tilde{h}_2$ in Eqn. (11)

$$\tilde{h}_i = -m'S(\tilde{r}_{cm})\tilde{V}_{o'} + [I']\tilde{\omega} - S(\tilde{r}_c)\tilde{P} \tag{17}$$

and differentiating with respect to time in the inertial frame yields the moment balance equation as follows.

$$\left.\frac{d\tilde{h}_i}{dt}\right|_I = \left.\frac{d}{dt}\right|_I \left(-m'S(\tilde{r}_{cm})\tilde{V}_{o'} + [I']\tilde{\omega}\right) - S(\tilde{V}_{o'})\tilde{P} - S(\tilde{r}_c)\left.\frac{d\tilde{P}}{dt}\right|_I \tag{18}$$

$$-\int_B S(\tilde{r}_c + \tilde{r})d\tilde{F} = \left.\frac{d}{dt}\right|_B \left(-m'S(\tilde{r}_{cm})\tilde{V}_{o'} + [I']\tilde{\omega}\right) - S(\tilde{\omega})[I']\tilde{\omega} + m'S(\tilde{\omega})S(\tilde{r}_{cm})\tilde{V}_{o'} - S(\tilde{V}_{o'})\left(m'\tilde{V}_{o'} - m'S(\tilde{\omega})\tilde{r}_{cm}\right) - S(\tilde{r}_c)\tilde{F} \tag{19}$$

$$-S(\tilde{r}_c)\tilde{F} + \tilde{M} = -m'S(\tilde{r}_{cm})\dot{\tilde{V}}_{o'_B} + [I']\dot{\tilde{\omega}} + m'S(\tilde{\omega})S(\tilde{r}_{cm})\tilde{V}_{o'} - S(\tilde{\omega})[I']\tilde{\omega} + m'S(\tilde{V}_{o'})S(\tilde{\omega})\tilde{r}_{cm} - S(\tilde{r}_c)\tilde{F} \tag{20}$$

$$-m'S(\tilde{r}_{cm})\dot{\tilde{V}}_{o'_B} + [I']\dot{\tilde{\omega}} = -m'S(\tilde{\omega})S(\tilde{r}_{cm})\tilde{V}_{o'} - m'S(\tilde{V}_{o'})S(\tilde{\omega})\tilde{r}_{cm} + S(\tilde{\omega})[I']\tilde{\omega} + \tilde{M} \tag{21}$$

where $\tilde{M}$ is the total external moment acting on the body about o'. The first two terms on the right hand side of Eqn. (21) can be further simplified using the vector triple product identity to yield

$$-m'S(\tilde{r}_{cm})\dot{\tilde{V}}_{o'_B} + [I']\dot{\tilde{\omega}} = m'S(\tilde{r}_{cm})S(\tilde{V}_{o'})\tilde{\omega} + S(\tilde{\omega})[I']\tilde{\omega} + \tilde{M} \tag{22}$$

Combining Eqns. (8) and (22) the complete asymmetric dynamics can be expressed in the matrix form as

$$\begin{bmatrix} \dot{u} \\ \dot{v} \\ \dot{w} \\ \dot{p} \\ \dot{q} \\ \dot{r} \end{bmatrix} = \begin{bmatrix} 1 & 0 & 0 & 0 & z_{cm} & -y_{cm} \\ 0 & 1 & 0 & -z_{cm} & 0 & x_{cm} \\ 0 & 0 & 1 & y_{cm} & -x_{cm} & 0 \\ 0 & -m'z_{cm} & m'y_{cm} & I'_{xx} & -I'_{xy} & -I'_{xz} \\ m'z_{cm} & 0 & -m'x_{cm} & -I'_{xy} & I'_{yy} & -I'_{yz} \\ -m'y_{cm} & m'x_{cm} & 0 & -I'_{xz} & -I'_{yz} & I'_{zz} \end{bmatrix}^{-1} \times \left(\begin{bmatrix} -qw + rv \\ -ru + pw \\ -pv + qu \\ I'_{xz}pq + (I'_{yy} - I'_{zz})qr - I'_{xy}rp + I'_{yz}(q^2 - r^2) \\ -I'_{yz}pq + I'_{xy}qr + (I'_{zz} - I'_{xx})rp + I'_{xz}(r^2 - p^2) \\ (I'_{xx} - I'_{yy})pq - I'_{xz}qr + I'_{yz}rp + I'_{xy}(p^2 - q^2) \end{bmatrix} + \begin{bmatrix} (q^2 + r^2)x_{cm} - pqy_{cm} - rpz_{cm} \\ -pqx_{cm} + (r^2 + p^2)y_{cm} - qrz_{cm} \\ -rpx_{cm} - qry_{cm} + (p^2 + q^2)z_{cm} \\ m'(qu - pv)y_{cm} + m'(ru - pw)z_{cm} \\ m'(pv - qu)x_{cm} + m'(rv - qw)z_{cm} \\ m'(pw - ru)x_{cm} + m'(qw - rv)y_{cm} \end{bmatrix} + \begin{bmatrix} \frac{1}{m'}F_x \\ \frac{1}{m'}F_y \\ \frac{1}{m'}F_z \\ M_x \\ M_y \\ M_z \end{bmatrix} \right) \tag{23}$$

The kinematic equations (both translational and rotational), however, remain unchanged. They are derived in any standard textbook on the subject[10,11]. Since the CG is away from the origin of the body frame, in addition to the usual aerodynamic and thrust components, there will appear a moment due to gravity component in the external moment given by

$$\tilde{M}_g = \begin{bmatrix} -z_{cm}m'g\cos\theta\sin\varphi + y_{cm}m'g\cos\theta\cos\varphi \\ -z_{cm}m'g\sin\theta - x_{cm}m'g\cos\theta\cos\varphi \\ y_{cm}m'g\sin\theta + x_{cm}m'g\cos\theta\sin\varphi \end{bmatrix} \tag{24}$$

where φ and θ are the roll and pitch body frame Euler angles. External force will have the usual aerodynamic, propulsive and gravity components.

2.2 Body Axes Fixed at the Shifted CG

As discussed earlier, alternate to the previous representation, 6-DOF equations of motion expressed in a body frame attached to the actual CG lying off the plane of symmetry can also be used to study the asymmetric dynamics of the aircraft. The schematic configuration is shown in Fig. 1(b). In this case, the force and moment balance equations reduce to

$$\dot{\tilde{V}}_{cm} = S(\tilde{\omega})\tilde{V}_{cm} + \frac{1}{m'}\tilde{F} \tag{25}$$

$$[I^{cm}]\dot{\tilde{\omega}} = S(\tilde{\omega})[I^{cm}]\tilde{\omega} + \tilde{M}' \tag{26}$$

where $\tilde{M}'$ is the external impressed moment vector which, unlike the previous model, will clearly have no gravity component as the origin of the body reference frame is at the CG itself. Linear velocity components will also differ from those as considered in the previous model. Breaking the above two equations in the components along the three new body

axes yields

$$\begin{bmatrix}\dot{u}'\\ \dot{v}'\\ \dot{w}'\end{bmatrix}=\begin{bmatrix}-qw'+rv'\\ -ru'+pw'\\ -pv'+qu'\end{bmatrix}+\frac{1}{m'}\begin{bmatrix}-m'g\sin\theta+F_X\\ m'g\cos\theta\sin\varphi+F_Y\\ m'g\cos\theta\cos\varphi+F_Z\end{bmatrix} \tag{27}$$

$$\begin{bmatrix}\dot{p}\\ \dot{q}\\ \dot{r}\end{bmatrix}=\begin{bmatrix}I_{xx}^{cm} & -I_{xy}^{cm} & -I_{xz}^{cm}\\ -I_{xy}^{cm} & I_{yy}^{cm} & -I_{yz}^{cm}\\ -I_{xz}^{cm} & -I_{yz}^{cm} & I_{zz}^{cm}\end{bmatrix}^{-1}\left(\begin{bmatrix}M'_X\\ M'_Y\\ M'_Z\end{bmatrix}+\begin{bmatrix}I_{xz}^{cm}pq+(I_{yy}^{cm}-I_{zz}^{cm})qr-I_{xy}^{cm}rp+I_{yz}^{cm}(q^2-r^2)\\ -I_{yz}^{cm}pq+I_{xy}^{cm}qr+(I_{zz}^{cm}-I_{xx}^{cm})rp+I_{xz}^{cm}(r^2-p^2)\\ (I_{xx}^{cm}-I_{yy}^{cm})pq-I_{xz}^{cm}qr+I_{yz}^{cm}rp+I_{xy}^{cm}(p^2-q^2)\end{bmatrix}\right) \tag{28}$$

The inertia matrix in the new body axes $[I^{cm}]$ can be easily computed from the inertia matrix about o' (as considered in the previous subsection) using the parallel axis theorem. The onboard inertial sensors usually give measurements about the nominal CG; therefore, the measurements need to be transformed to the new body axes. The linear velocity components in this new body frame can be obtained from the corresponding measurements in the frame attached to the point o' by combining the accelerometer and gyro outputs using Eqn. (1) as

$$\begin{bmatrix}u'\\ v'\\ w'\end{bmatrix}=\begin{bmatrix}u\\ v\\ w\end{bmatrix}+\begin{bmatrix}0 & z_{cm} & -y_{cm}\\ -z_{cm} & 0 & x_{cm}\\ y_{cm} & -x_{cm} & 0\end{bmatrix}\begin{bmatrix}p\\ q\\ r\end{bmatrix} \tag{29}$$

Angular velocity measurements, however, remain the same in both the frames. It may be noted that the aerodynamic forces and moments should be computed from the AOA and sideslip angles at the nominal point o' and not about this new shifted CG since the aerodynamics of the aircraft does not depend on the CG location of the aircraft, it depends only on its geometric configuration. Like the previous model, the kinematic equations again remain unchanged.

3. CONTROL DESIGN FOR HERBST MANOEUVER: WITHOUT CG OFFSET

In the post stall regime, the aircraft dynamics becomes highly nonlinear and coupled. Moreover, an aggressive manoeuver demands high angular rates to be generated. Such extreme conditions call for use of nonlinear control techniques as gain scheduled linear controls become ineffective. Nonlinear dynamic inversion (NDI) or feedback linearising control is a popular nonlinear control design technique which has been applied to flight control problems by various researchers[5-8]. The basic underlying idea of this method is to first choose linear asymptotically stable error dynamics and then replace the system dynamics in it and solve for the control input. In flight control, this is realised in two steps using the inner loop – outer loop architecture as shown in Fig. 2 to exploit the inherent two time scale separation of the aircraft flight dynamics.

The outer loop control involves the slow angular variables (such as α,β,μ) and treats the fast variables, which are generally the angular rates as the virtual controls. The inner loop control ensures that suitable moments are generated so that the actual

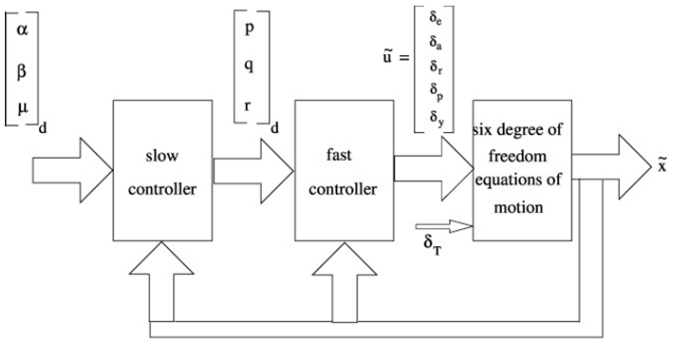

Figure 2. Block diagram of the closed loop control scheme.

angular rates match the rates as commanded by the outer loop controller. Control surface deflections are finally obtained from these moments using some control allocation algorithm. This two time scale approach along with the reasonable assumption that the control surfaces only generate moments without producing any appreciable force, help avoid the occurrence of internal dynamics, whose stability is the main challenge in the NDI algorithm[5,8,15] .

Let us first design the control for simulation implementation of Herbst manoeuver under the nominal condition i.e., no CG variation. Let this controller be denoted as the Nominal NDI control. Availability of state feedback is assumed for implementation of the scheme. For the outer loop controller, a linear asymptotically stable error dynamics is chosen element wise as

$$(\dot{a}_d-\dot{a})+k_{1a}(a_d-a)+k_{2a}\int(a_d-a)\,dt=0 \qquad for\ \ a=\alpha,\beta,\mu \tag{30}$$

where k_{1a} and k_{2a} are positive constants and the subscript d denotes the desired value. On substitution of the expressions for $\dot{a}$ $(i.e.\ \dot{\alpha},\dot{\beta},\dot{\mu})$ from the standard aircraft dynamics (as given in the appendix) into Eqn. (30) and after rearrangement, the desired body rates are obtained as

$$\begin{bmatrix}p_d\\ q_d\\ r_d\end{bmatrix}=\begin{bmatrix}-\cos\alpha\tan\beta & 1 & -\sin\alpha\tan\beta\\ \sin\alpha & 0 & -\cos\alpha\\ \cos\alpha\sec\beta & 0 & \sin\alpha\sec\beta\end{bmatrix}^{-1}\times$$

$$\left(\begin{bmatrix}\dot{\alpha}_d+k_{1\alpha}(\alpha_d-\alpha)+k_{2\alpha}\int(\alpha_d-\alpha)\,dt\\ \dot{\beta}_d+k_{1\beta}(\beta_d-\beta)+k_{2\beta}\int(\beta_d-\beta)\,dt\\ \dot{\mu}_d+k_{1\mu}(\mu_d-\mu)+k_{2\mu}\int(\mu_d-\mu)\,dt\end{bmatrix}-\frac{g}{V}\begin{bmatrix}\sec\beta\cos\mu\cos\gamma\\ \sin\mu\cos\gamma\\ -\tan\beta\cos\mu\cos\gamma\end{bmatrix}\right.$$

$$\left.-\frac{1}{mV}\begin{bmatrix}\sec\beta\,F_z^w\\ F_Y^w\\ \tan\gamma\cos\mu\,F_Y^w-(\tan\beta+\sin\mu\tan\gamma)F_Z^w\end{bmatrix}\right) \tag{31}$$

where the notations are defined in the appendix. Similarly, for the inner loop, the error dynamics is chosen element wise as

$$(\dot{c}_d-\dot{c})+k_{1c}(c_d-c)+k_{2c}\int(c_d-c)\,dt=0 \qquad for\ \ c=p,q,r \tag{32}$$

where k_{1c} and k_{2c} are positive constants so chosen that the error dynamics is asymptotically stable. After substitution of the expressions for $\dot{c}$ $(i.e.\ \dot{p},\dot{q},\dot{r})$ from the appendix to Eqn. (32)

and after rearrangement, the required control moments along the three body axes are obtained as

$$\begin{bmatrix} M_X \\ M_Y \\ M_Z \end{bmatrix}_C = \begin{bmatrix} I_{xx} & 0 & -I_{xz} \\ 0 & I_{yy} & 0 \\ -I_{xz} & 0 & I_{zz} \end{bmatrix} \begin{bmatrix} \dot{p}_d + k_{1p}(p_d - p) + k_{2p}\int (p_d - p)\,dt \\ \dot{q}_d + k_{1q}(q_d - q) + k_{2q}\int (q_d - q)\,dt \\ \dot{r}_d + k_{1r}(r_d - r) + k_{2r}\int (r_d - r)\,dt \end{bmatrix}$$

$$- \begin{bmatrix} (I_{yy} - I_{zz})qr + I_{xz}pq \\ (I_{zz} - I_{xx})rp + I_{xz}(r^2 - p^2) \\ (I_{xx} - I_{yy})pq - I_{xz}qr \end{bmatrix} - \begin{bmatrix} M_X \\ M_Y \\ M_Z \end{bmatrix}_S \tag{33}$$

where $\begin{bmatrix} M_x & M_y & M_z \end{bmatrix}_S^T$ and $\begin{bmatrix} M_x & M_y & M_z \end{bmatrix}_C^T$ denote the state and control dependent parts of the external moment vector respectively. From Eqn. (33) final control surface deflections can be computed using the matrix pseudo inverse method of control allocation as outlined in the literature[5].

4. CONTROL DESIGN UNDER LATERAL CG VARIATION

NDI control formulation based on the two models for asymmetric 6-DOF dynamics as derived in Section 2 are presented considering that the aircraft has undergone lateral CG movement from asymmetric firing of stores. Let the two formulations corresponding to the two models be denoted as Modified NDI-1 and Modified NDI-2 control schemes.

4.1 Modified NDI-1 Scheme

First let us consider the asymmetric dynamics to be expressed in the body frame fixed at the nominal CG location in the plane of symmetry. The force and moment balance equations (i.e., Eqns. (8) and (22) can be expressed in matrix format as

$$\begin{bmatrix} 1 & 0 & 0 & 0 & z_{cm} & -y_{cm} \\ 0 & 1 & 0 & -z_{cm} & 0 & x_{cm} \\ 0 & 0 & 1 & y_{cm} & -x_{cm} & 0 \end{bmatrix} \begin{bmatrix} \dot{u} \\ \dot{v} \\ \dot{w} \\ \dot{p} \\ \dot{q} \\ \dot{r} \end{bmatrix} = \frac{1}{m'} \begin{bmatrix} F_x \\ F_y \\ F_z \end{bmatrix} +$$

$$\begin{bmatrix} -qw + rv + (q^2 + r^2)x_{cm} - pqy_{cm} - rpz_{cm} \\ -ru + pw + (r^2 + p^2)y_{cm} - pqx_{cm} - qrz_{cm} \\ -pv + qu + (p^2 + q^2)z_{cm} - rpx_{cm} - qry_{cm} \end{bmatrix} \tag{34}$$

$$\begin{bmatrix} 0 & -m'z_{cm} & m'y_{cm} & I'_{xx} & -I'_{xy} & -I'_{xz} \\ m'z_{cm} & 0 & -m'x_{cm} & -I'_{xy} & I'_{yy} & -I'_{yz} \\ -m'y_{cm} & m'x_{cm} & 0 & -I'_{xz} & -I'_{yz} & I'_{zz} \end{bmatrix} \begin{bmatrix} \dot{u} \\ \dot{v} \\ \dot{w} \\ \dot{p} \\ \dot{q} \\ \dot{r} \end{bmatrix} =$$

$$\begin{bmatrix} I'_{xz}pq + (I'_{yy} - I'_{zz})qr - I'_{xy}rp + I'_{yz}(q^2 - r^2) \\ -I'_{yz}pq + I'_{xy}qr + (I'_{zz} - I'_{xx})rp + I'_{xz}(r^2 - p^2) \\ (I'_{xx} - I'_{yy})pq - I'_{xz}qr + I'_{yz}rp + I'_{xy}(p^2 - q^2) \end{bmatrix} +$$

$$\begin{bmatrix} m'(qu - pv)y_{cm} + m'(ru - pw)z_{cm} \\ m'(pv - qu)x_{cm} + m'(rv - qw)z_{cm} \\ m'(pw - ru)x_{cm} + m'(qw - rv)y_{cm} \end{bmatrix} + \begin{bmatrix} M_x \\ M_y \\ M_z \end{bmatrix} \tag{35}$$

From the above equations the linear and angular accelerations can be separated as

$$\begin{bmatrix} \dot{u} \\ \dot{v} \\ \dot{w} \end{bmatrix} = \frac{1}{m'}[A]\left(\frac{1}{m'}[A^2] + [I']\right)^{-1}\left(-[A]\begin{bmatrix} F_1 \\ F_2 \\ F_3 \end{bmatrix} - \frac{1}{m'}[A]\begin{bmatrix} F_x \\ F_y \\ F_z \end{bmatrix}\right.$$

$$\left. + \begin{bmatrix} M_1 \\ M_2 \\ M_3 \end{bmatrix} + \begin{bmatrix} M_x \\ M_y \\ M_z \end{bmatrix}_S + \begin{bmatrix} M_x \\ M_y \\ M_z \end{bmatrix}_C\right) + \begin{bmatrix} F_1 \\ F_2 \\ F_3 \end{bmatrix} + \frac{1}{m'}\begin{bmatrix} F_x \\ F_y \\ F_z \end{bmatrix} \tag{36}$$

$$\begin{bmatrix} \dot{p} \\ \dot{q} \\ \dot{r} \end{bmatrix} = \left(\frac{1}{m'}[A^2] + [I']\right)^{-1}\left(-[A]\begin{bmatrix} F_1 \\ F_2 \\ F_3 \end{bmatrix} - \frac{1}{m'}[A]\begin{bmatrix} F_x \\ F_y \\ F_z \end{bmatrix} + \begin{bmatrix} M_1 \\ M_2 \\ M_3 \end{bmatrix}\right.$$

$$\left. + \begin{bmatrix} M_x \\ M_y \\ M_z \end{bmatrix}_S + \begin{bmatrix} M_x \\ M_y \\ M_z \end{bmatrix}_C\right) \tag{37}$$

where as stated earlier, $\begin{bmatrix} M_x & M_y & M_z \end{bmatrix}_S^T$ and $\begin{bmatrix} M_x & M_y & M_z \end{bmatrix}_C^T$ denote the state and control dependent parts of the external moment vector respectively; $\begin{bmatrix} F_1 & F_2 & F_3 \end{bmatrix}^T$ denotes the first term on the right hand side of Eqn (34); $\begin{bmatrix} M_1 & M_2 & M_3 \end{bmatrix}^T$ denotes the first two terms on the right hand side of Eqn. (35) and

$$[A] \triangleq \begin{bmatrix} 0 & -m'z_{cm} & m'y_{cm} \\ m'z_{cm} & 0 & -m'x_{cm} \\ -m'y_{cm} & m'x_{cm} & 0 \end{bmatrix} \tag{38}$$

For control design purpose it is assumed that the control deflections produce only moments; therefore, they do not affect the linear accelerations. Hence, Eqn. (36) can be approximated as

$$\begin{bmatrix} \dot{u} \\ \dot{v} \\ \dot{w} \end{bmatrix} = \frac{1}{m'}[A]\left(\frac{1}{m'}[A^2] + [I']\right)^{-1}\left(-[A]\begin{bmatrix} F_1 \\ F_2 \\ F_3 \end{bmatrix} - \frac{1}{m'}[A]\begin{bmatrix} F_x \\ F_y \\ F_z \end{bmatrix}\right.$$

$$\left. + \begin{bmatrix} M_1 \\ M_2 \\ M_3 \end{bmatrix} + \begin{bmatrix} M_x \\ M_y \\ M_z \end{bmatrix}_S\right) + \begin{bmatrix} F_1 \\ F_2 \\ F_3 \end{bmatrix} + \frac{1}{m'}\begin{bmatrix} F_x \\ F_y \\ F_z \end{bmatrix} \tag{39}$$

It can be shown[11] that the relations between the wind axis aerodynamic angle rates $(\dot{\alpha}, \dot{\beta}, \dot{\mu})$ and the body axis linear accelerations $(\dot{u}, \dot{v}, \dot{w})$ can be expressed in a compact form as

$$\begin{bmatrix} \dot{\alpha} \\ \dot{\beta} \\ \dot{\mu} \end{bmatrix} = \begin{bmatrix} 0 & 0 & 0 & 0 & 0 \\ 0 & 0 & 0 & 0 & 0 \\ 0 & 0 & 1 & tan\gamma\, sin\mu & tan\gamma\, cos\mu \end{bmatrix}$$

$$\begin{bmatrix} 0 & 0 & 0 & 0 & 0 \\ 0 & 0 & 0 & 0 & 0 \\ 0 & 0 & cos\alpha\, cos\beta & sin\beta & sin\alpha\, cos\beta \\ 0 & 0 & -cos\alpha\, sin\beta & cos\beta & -sin\alpha\, sin\beta \\ 0 & 0 & -sin\alpha & 0 & cos\alpha \end{bmatrix} \left(\begin{bmatrix} 0 \\ 0 \\ p \\ q \\ r \end{bmatrix} - \frac{1}{V} \times \right.$$

$$\left. \begin{bmatrix} -sin\alpha sec\beta & 0 & cos\alpha sec\beta \\ -cos\alpha sin\beta & cos\beta & -sin\alpha sin\beta \\ -sin\alpha cos\alpha sec\beta & sin\alpha cos\beta & -sin^2\alpha sin\beta \\ -sin\alpha sec\beta & 0 & cos\alpha sec\beta \\ cos^2\alpha sin\beta & -cos\alpha cos\beta & sin\alpha cos\alpha sin\beta \end{bmatrix} \begin{bmatrix} \dot{u} \\ \dot{v} \\ \dot{w} \end{bmatrix} \right) \quad (40)$$

For a stable error dynamics for the outer loop, Eqn. (30) is rearranged as

$$\begin{bmatrix} \dot{\alpha} \\ \dot{\beta} \\ \dot{\mu} \end{bmatrix} = \begin{bmatrix} \dot{\alpha}_d + k_{1\alpha}(\alpha_d - \alpha) + k_{2\alpha}\int(\alpha_d - \alpha)dt \\ \dot{\beta}_d + k_{1\beta}(\beta_d - \beta) + k_{2\beta}\int(\beta_d - \beta)dt \\ \dot{\mu}_d + k_{1\mu}(\mu_d - \mu) + k_{2\mu}\int(\mu_d - \mu)dt \end{bmatrix} \quad (41)$$

where the right hand side is known at every time step. Substituting $[\dot{u}\ \dot{v}\ \dot{w}]^T$ from Eqn. (39) into Eqn. (40) and then substituting the resulting $[\dot{\alpha}\ \dot{\beta}\ \dot{\mu}]^T$ equation on the left hand side of Eqn. (41) gives implicit equations for $[p\ q\ r]^T$, which are solved numerically to compute the desired body rates $[p_d\ q_d\ r_d]^T$. As Eqn. (39) contains product and square nonlinearities involving *p, q,* and *r,* the solution is obtained iteratively. The values of $[p_d\ q_d\ r_d]^T$ thus estimated numerically from the outer loop controller are fed to the inner loop controller which needs to satisfy the following equation for a stable error dynamics for the body rates

$$\begin{bmatrix} \dot{p} \\ \dot{q} \\ \dot{r} \end{bmatrix} = \begin{bmatrix} \dot{p}_d + k_{1p}(p_d - p) + k_{2p}\int(p_d - p)dt \\ \dot{q}_d + k_{1q}(q_d - q) + k_{2q}\int(q_d - q)dt \\ \dot{r}_d + k_{1r}(r_d - r) + k_{2r}\int(r_d - r)dt \end{bmatrix} \quad (42)$$

The right hand side of Eqn. (42) is again known at every time step. Inserting Eqn. (37) in the left hand side of Eqn. (42) the commanded control moments $[M_x\ \ M_y\ \ M_z]_C^T$ can be computed as

$$\begin{bmatrix} M_x \\ M_y \\ M_z \end{bmatrix}_C = \left(\frac{1}{m'}[A^2] + [I'] \right) \begin{bmatrix} \dot{p}_d + k_{1p}(p_d - p) + k_{2p}\int(p_d - p)dt \\ \dot{q}_d + k_{1q}(q_d - q) + k_{2q}\int(q_d - q)dt \\ \dot{r}_d + k_{1r}(r_d - r) + k_{2r}\int(r_d - r)dt \end{bmatrix}$$

$$+ [A] \begin{bmatrix} F_1 \\ F_2 \\ F_3 \end{bmatrix} + \frac{1}{m'}[A] \begin{bmatrix} F_x \\ F_y \\ F_z \end{bmatrix} - \begin{bmatrix} M_1 \\ M_2 \\ M_3 \end{bmatrix} - \begin{bmatrix} M_x \\ M_y \\ M_z \end{bmatrix}_S \quad (43)$$

from which the control surface deflections are finally obtained through the matrix pseudo inverse method as mentioned in the previous section.

4.2 Modified NDI-2 Scheme

We now consider the asymmetric dynamics to be expressed in the frame attached to the actual offset CG location for the closed loop control design purpose. As discussed earlier, the asymmetric 6-DOF dynamics, in this case, is described by Eqns. (27) and (28) which are very similar to the equations for the standard symmetric dynamics except for the fact that the linear accelerations are now different. Therefore, if the measurements of the linear velocity components are transformed to this new frame using Eqn. (29), then the dynamics expressed in terms of $[u'\ v'\ w']^T$ (and hence in terms of (α', β') can be directly used by the controller the same way as the Nominal NDI controller as discussed in Section 3. However, the desired values of α' and β' are not known beforehand since they depend on the desired values of *p, q,* and *r* which are only computed online. Therefore, instead of feeding α'_d, β'_d and μ'_d to the outer loop, α_d, β_d and μ_d profiles as considered in the previous two schemes are fed. Moreover, for control computations, the aerodynamic forces and moments are computed from the tables based on α and β and not α' and β'.

5. RESULTS AND DISCUSSIONS

In Herbst manoeuver, the aircraft is first made to pitch up to a sufficiently high AOA (about 60°-70°) and thereafter is commanded to bank to a high angle at a high rate to initiate a quick turn. This is followed by returning the AOA and the bank angle to the initial values after a few seconds. This help the aircraft rapidly reverse its flight direction and therefore, quickly return to the base after performing some combat mission[12-13]. Recently, a Herbst like manoeuver has been implemented for micro aerial vehicles also for smooth navigation through a forest[14]. To simulate the manoeuver using the nominal NDI control under zero CG offset, suitable bell-shaped desired profile are considered for AOA and bank angle for a total manoeuver time of 18 *s* starting at *t* = 5*s*. Sideslip angle is commanded to remain zero throughout. Before initiating the manoeuver the aircraft was assumed to be trimmed at 0.6*Mach* and at an altitude of 3000 *m*. A typical fighter aircraft has been considered possessing thrust vector control in both pitch and yaw planes along with the conventional controls, namely stabilator, aileron, rudder and throttle. However, throttle is controlled separately in an open loop fashion. All the surfaces are limited by positions and rate saturations as given in Table 1. Various control parameters (as in Eqns. (30) and (32)) which are designed by trial and error are k_{1a}, k_{2a} = *diag* (4.0, 2.0, 2.0) and k_{1c}, k_{2c} = *diag* (0.05, 0.01, 0.05). On a 3.1GHz Intel-i7 processor with Windows7 Professional operating system, the simulation, when run in MATLAB R2014a, took about 60*s* for a step size of 25 ms. Figure 3 shows excellent tracking of the commanded profiles with negligible sideslip buildup and with the controls staying well within their respective saturation limits. As bank angle goes beyond 90°, lift acts downwards for some time thereby causing sharp altitude drop. However, the pilot can easily recover the aircraft from such a situation once

Table 1. Saturation levels of the control surfaces

Limits	Stabilator	Aileron	Rudder	Pitch nozzle	Yaw nozzle
Position	± 25°	± 25°	± 25°	± 20°	± 20°
Rate	± 60°/s	± 90°/s	± 90°/s	± 80°/s	± 80°/s

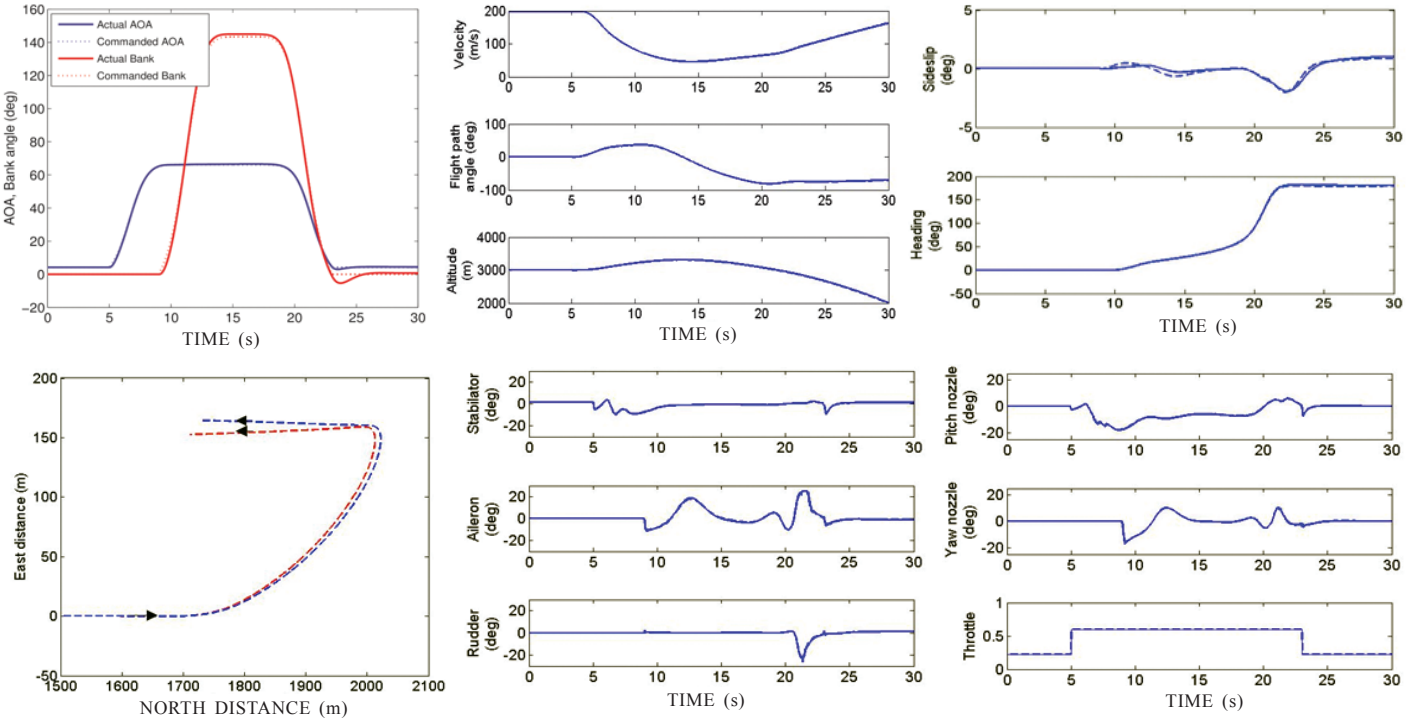

Figure 3. Time response and control profiles for Herbst manoeuver for nominal CG location.

the manoeuver is complete. Figure 3 shows two sets of plots corresponding to two sets of aerodynamic data as considered by the controller - one the actual experimental data and the other representing a modest ± 5 per cent random uncertainty in the data. Several simulation runs were carried out and the scheme was observed to function properly within the aforementioned uncertainty band. One such sample results are shown in Fig. 3 along with the zero aerodynamic uncertainty case and, as can be observed therein, both the plots are almost overlapping. However, it was also observed that the manoeuver performance started to get considerably affected once a higher uncertainty level (about ± 10 per cent) is imposed on the aerodynamic dataset.

To simulate the performance of the control scheme under lateral CG variation, the aircraft is assumed to initially carry two identical stores weighing 500 kg each located at a lateral distance of 176 cm on either side from its plane of symmetry and a vertically downward distance of 45 cm from the nominal CG location o'. The store under the port wing is assumed to be released 1*s* prior to the initiation of the manoeuver. The initial trim and the pole locations corresponding to both inner and outer loop error dynamics are taken to be the same as considered before. Time simulations as shown in Figure 4 compare the performance of the nominal NDI controller and the proposed modified NDI-1 controller under the given CG offset. From this figure it is observed that, while the nominal NDI controller performance gets drastically affected, the modified NDI-1 controller is able to maintain almost the same level of performance as the nominal case of no lateral CG offset. However, because of the more complex computations involved, the modified NDI-1 controller is found to require about 12 per cent - 15 per cent higher computation time when simulated using the same computational facility as mentioned before.

The time response for Herbst manoeuver using the modified NDI-2 control formulation is shown and compared with the performance of the nominal NDI control in Fig. 5 under the same lateral CG offset as considered previously. From this figure it is observed that the modified NDI-2 controller achieves almost complete insensitivity to the given amount of lateral CG variation. As expected, the performance of modified NDI-1 and of modified NDI-2 controls are very similar. This is because the system dynamics they consider for their respective control computations are equivalent. As no extra computational complexity is invited unlike the modified NDI-1 control formulation, no increase in simulation time as compared to the nominal NDI control scheme is observed in the present scheme. Moreover, both of the proposed control schemes were found to be tolerant to the same ± 5 per cent uncertainty level in the aerodynamic coefficients as considered before.

6. CONCLUSIONS

The effects of lateral CG movement arising from asymmetric firing of onboard stores on post-stall manoeuvers such as the Herbst was found to be quite significant as observed through explicit modelling of 6 DOF aircraft equations of motion from the first principle about two different body reference frames and carrying out dynamic inversion based nonlinear control design. It was observed that even a modest lateral CG offset may lead to lateral-directional control saturation when such a demanding manoeuver involving extreme motions in both longitudinal and lateral-directional planes is attempted which, in turn, may significantly worsen the manoeuver performance. Incorporating the derived asymmetric equations of motion into the control formulation helped regain the lost manoeuver performance significantly. However, it

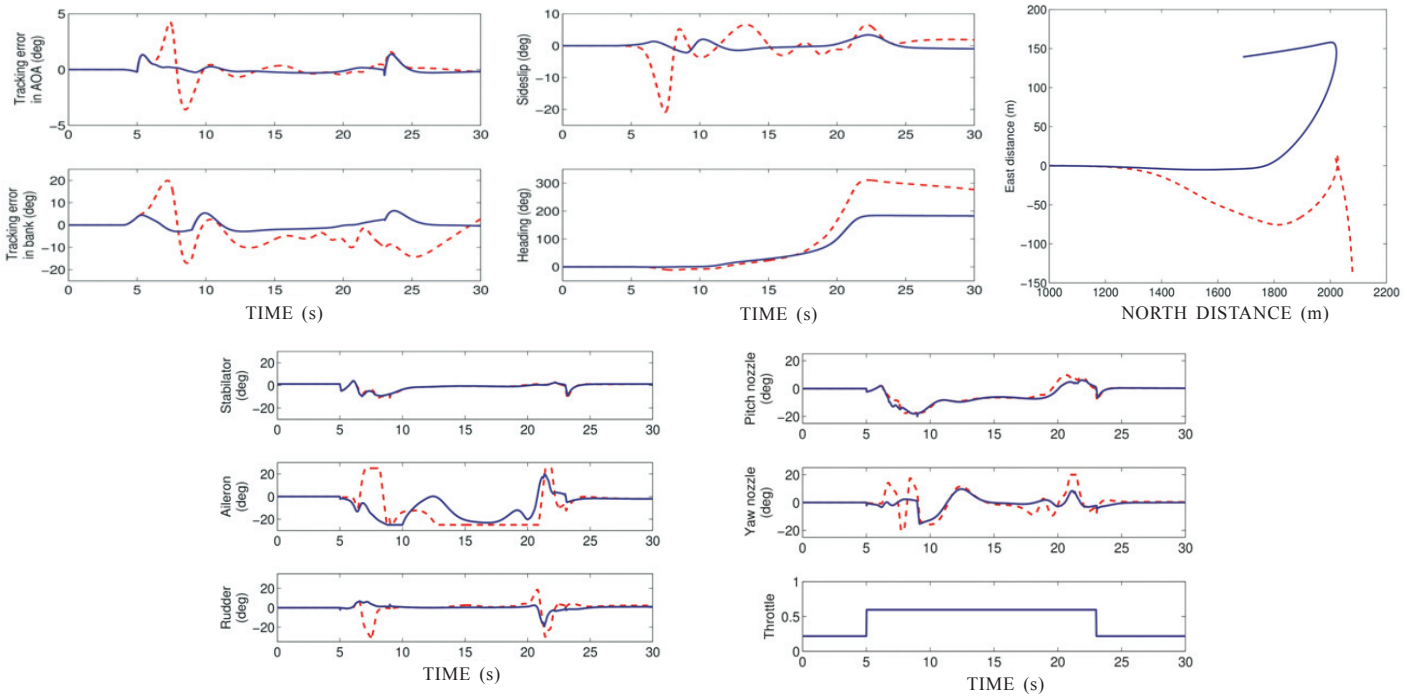

Figure 4. Departure in Herbst manoeuver performance due to the lateral CG shift (- - Nominal NDI, -- Modified NDI-1).

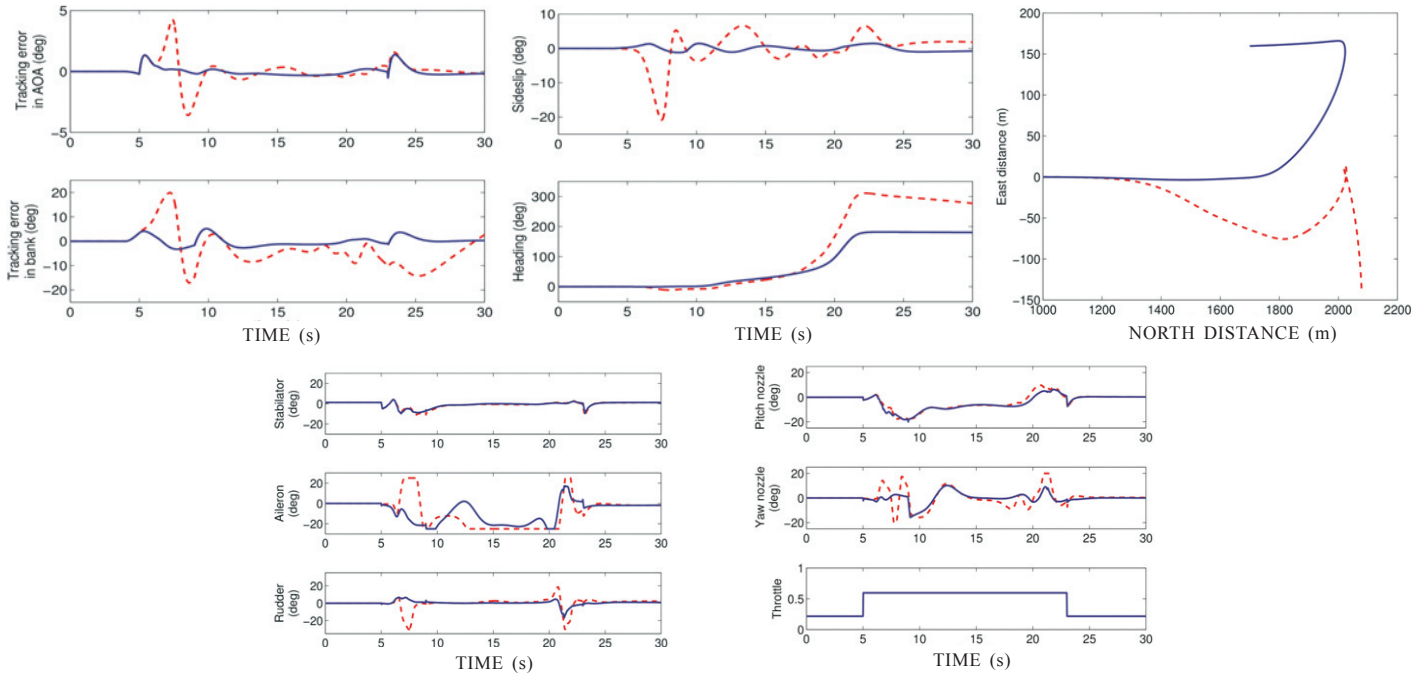

Figure 5. Departure in Herbst manoeuver performance due to the lateral CG shift (- - Nominal NDI, -- Modified NDI-2).

was achieved at a cost of either some increase in computation burden or transformation of the measurements and defining the state variables at a new reference frame.

REFERENCES

1. Bacon, B.J. & Gregory, I.M. General equations of motion for a damaged asymmetric aircraft. *In* Proceedings of the AIAA Atmospheric Flight Mechanics Conference and Exhibits, South California, USA, 20-23 August 2007.
2. Nguyen, N.; Krishnakumar, K.; Kaneshige, J. & Nespeca, P. Flight dynamics and hybrid adaptive control of damaged aircraft. *J. Guid. Control Dyn.*, 2008, **31**(5), 751-764. doi: 10.2514/1.28142
3. Liu, Y.; Tao, G. & Joshi, S.M. Modeling and model reference adaptive control of aircraft with asymmetric damage. *J. Guid. Control Dyn.*, 2010, **33**(5), 1500-1517. doi: 10.2514/1.47996
4. Guo, J.; Tao, G. & Liu, Y. Multivariable adaptive control of NASA generic transport aircraft model with damage. *J. Guid. Control Dyn.*, 2011, **34**(5), 1495-1506. doi: 10.2514/1.53258
5. Snell, S.A; Enns, D.F. & Garrard Jr., W.L. Nonlinear

inversion flight control for a super manoeuverable aircraft. *J. Guid. Control Dyn*, 1992, **15**(4), 976-984. doi: 10.2514/3.20932

6. Khatri, A.K.; Singh, J. & Sinha, N.K. Accessible Regions for Controlled Aircraft Manoeuvering. *J. Guid. Control Dyn.,* 2013, **36**(6), 1829-1834. doi: 10.2514/1.59592
7. Singh, S.N. Asymptotically decoupled discontinuous control of systems and nonlinear aircraft manoeuver. *IEEE Trans. Aerosp. Electron. Syst.*, 1989, **25**(3), 380-391. doi: 10.1109/ 7.30793.
8. Lane, S.H. & Stengel, R.F. Flight control design using nonlinear inverse dynamics. *Automatica*, 1988, **24**(4), 471-483. doi:10.1016/0005-1098 (88) 90092-1.
9. Bugajski, D.J.; Enns, D.F. & Garrard Jr., W.L. Nonlinear control law with application to high angle-of-attack flight, *J. Guid. Control Dyn.*, 1992, **15**(3), 761-767. doi: 10.2514/3.20902
10. Etkin, B. Dynamics of atmospheric flight. Dover Publications Inc., New York, 2005.
11. Stevens, B.L. & Lewis, F.L. Aircraft control and simulation., Wiley India Pvt. Ltd., India, 2003.
12. Pourtakdoust, S.H.; Karimi, J. & Shajiee. Design of a tracking control system for an optimal post-stall manoeuver using dynamic inversion approach. *In* Proceedings of the 25th International Congress of Aeronautical Sciences, Hamburg, Germany, 3-8 September 2006.
13. Chiang, R.Y.; Safonov, M.G.; Haiges, K.; Madden, K. & Tekawt, J. A fixed H^{∞} controller for a supermanoeuverable fighter performing the herbst manoeuver. *Automatica*, 1993, **29**(1), 111-127. doi:10.1016/0005-1098(93)90176-t
14. Paranjape, A.A.; Mier, K.C.; Shi, X.; Chung, S. & Hutchinson, S. Motion primitives and 3D path planning for fast flight through a forest. *Int. J. Robot Res.*, 2015, **34**(3), 357-377. doi: 10.1177/ 0278364914558017
15. Slotine, J.J.E. & Li, W. Applied nonlinear control. Prentice-Hall, New Jersey, 1991.

CONTRIBUTORS

Mr Bijoy K. Mukherjee received his BE (Electrical Engineering) from North Bengal University, India and ME (Control Systems) from IIEST Shibpur, India. Currently pursuing his PhD from the Department of Aerospace Engineering, IIT Kharagpur, India. His current research interests include : Aircraft flight control and spacecraft attitude control using nonlinear, adaptive and intelligent control techniques.
In the current study, he has carried out the experiment, done analysis, and prepared the manuscript.

Dr Manoranjan Sinha received his BTech (Civil Engineering) from IIT Delhi, India and MTech and PhD in Aerospace Engineering from IIT Kanpur, India. Presently working as an Associate Professor at the Department of Aerospace Engineering, IIT Kharagpur, India. His research interests include : Flight dynamics, space dynamics, control systems, system identification and artificial neural networks.
In the current study, he has provided the guidance and supervision.

Appendix

Standard Aircraft Dynamics

Following are the standard 6-DOF dynamic model of a rigid aircraft (valid under the assumptions of constant aircraft mass and a flat non-rotating Earth) expressed in the body axes.

$$\begin{bmatrix}\dot{u}\\ \dot{v}\\ \dot{w}\end{bmatrix}=\begin{bmatrix}-qw+rv\\ -ru+pw\\ -pv+qu\end{bmatrix}+\frac{1}{m}\begin{bmatrix}-mg\sin\theta+F_X\\ mg\cos\theta\sin\varphi+F_Y\\ mg\cos\theta\cos\varphi+F_Z\end{bmatrix}$$

$$\begin{bmatrix}I_{xx} & 0 & -I_{xz}\\ 0 & I_{yy} & 0\\ -I_{xz} & 0 & I_{zz}\end{bmatrix}\begin{bmatrix}\dot{p}\\ \dot{q}\\ \dot{r}\end{bmatrix}=\begin{bmatrix}(I_{yy}-I_{zz})qr+I_{xz}pq\\ (I_{zz}-I_{xx})rp+I_{xz}(r^2-p^2)\\ (I_{xx}-I_{yy})pq-I_{xz}qr\end{bmatrix}+\begin{bmatrix}M_X\\ M_Y\\ M_Z\end{bmatrix}$$

Following 6-DOF dynamics in wind axes can be derived from any standard textbook on aircraft flight dynamics[11].

$$\begin{bmatrix}\dot{V}\\ \dot{\gamma}\\ \dot{\chi}\end{bmatrix}=\begin{bmatrix}-g\sin\gamma+\frac{1}{m}F_X^w\\ -\frac{g}{V}\cos\gamma-\frac{1}{mV}\sin\mu\,F_Y^w-\frac{1}{mV}\cos\mu\,F_z^w\\ \frac{1}{mV}\cos\mu\sec\gamma\,F_Y^w-\frac{1}{mV}\sin\mu\sec\gamma\,F_z^w\end{bmatrix}$$

$$\begin{bmatrix}\dot{\alpha}\\ \dot{\beta}\\ \dot{\mu}\end{bmatrix}=\begin{bmatrix}q-p\cos\alpha\tan\beta-r\sin\alpha\tan\beta\\ p\sin\alpha-r\cos\alpha\\ p\cos\alpha\sec\beta+r\sin\alpha\sec\beta\end{bmatrix}+\frac{g}{V}\begin{bmatrix}\sec\beta\cos\mu\cos\gamma\\ \sin\mu\cos\gamma\\ -\tan\beta\cos\mu\cos\gamma\end{bmatrix}$$

$$+\frac{1}{m\,V}\begin{bmatrix}\sec\beta\,F_Z^w\\ F_Y^w\\ \tan\gamma\cos\mu\,F_Y^w-\left(\tan\beta+\sin\mu\tan\gamma\right)F_Z^w\end{bmatrix}$$

where

$$\begin{bmatrix}F_X^w\\ F_Y^w\\ F_Z^w\end{bmatrix}=\begin{bmatrix}\cos\alpha\cos\beta & \sin\beta & \sin\alpha\cos\beta\\ -\cos\alpha\sin\beta & \cos\beta & -\sin\alpha\sin\beta\\ -\sin\alpha & 0 & \cos\alpha\end{bmatrix}\begin{bmatrix}F_X\\ F_Y\\ F_Z\end{bmatrix}$$

denotes the aerodynamic and propulsive forces resolved along the wind axes.